Phase-Shift High-Speed Valve for Switch-Mode Control

James D. Van de Ven
e-mail: vandeven@wpi.edu

Allan Katz
e-mail: akatz@wpi.edu

Department of Mechanical Engineering,
Worcester Polytechnic Institute,
100 Institute Road,
Worcester, MA 01609

Hydraulic applications requiring a variation in the speed or torque of actuators have historically used throttling valve control or a variable displacement pump or motor. An alternative method is switch-mode control that uses a high-speed valve to rapidly switch between efficient on and off states, allowing any hydraulic actuator to have virtually variable displacement. An existing barrier to switch-mode control is a fast and efficient high-speed valve. A novel high-speed valve concept is proposed that uses a phase shift between two tiers of continuously rotating valve spools to achieve a pulse-width modulated flow with any desired duty ratio. An analysis of the major forms of energy loss, including throttling, compressibility, viscous friction, and internal leakage, is performed on a disk spool architecture. This analysis also explores the use of a hydrodynamic thrust bearing to maintain valve clearance. A nonoptimized design example of a phase-shift valve operating at 100 Hz switching frequency at 10 l/min demonstrates an efficiency of 73% at a duty ratio of 1 and 64% at 0.75 duty ratio. Numerous opportunities exist for improving this efficiency including design changes and formal optimization. The phase-shift valve has the potential to enable switch-mode hydraulic circuits. The valve has numerous benefits over existing technology yet requires further refinement to realize its full potential. [DOI: 10.1115/1.4002706]

Keywords: switch-mode hydraulics, on-off valve, PWM hydraulics, virtually variable displacement, four-quadrant operation

1 Introduction and Background

In numerous hydraulic applications, there is a need for varying the speed and torque or force of rotary and linear hydraulic actuators. This can be accomplished by throttling flow across a valve, by using variable displacement pumps or motors, or by using switch-mode valve control. Throttling flow wastes energy and creates heat, while adding variable displacement capability to a pump or motor adds weight, volume, and expense [1]. Additionally, few pump/motor units are capable of both positive and negative displacement, as is necessary for regenerative braking in applications such as a hydraulic hybrid vehicle. Furthermore, mechanical displacement control cannot be easily implemented in some pump/motor architectures, such as gear, radial piston, and gerotor.

To achieve virtual variable displacement control of hydraulic components, a switch-mode hydraulic circuit, the hydraulic analog of a switch-mode power supply, is proposed [2]. This concept, previously applied to hydraulic transformers [3], pumps [1,4–6], linear actuators [7], engine valves [8], and multiple actuators [9], utilizes a high-speed switching valve to switch between efficient on and off states. By setting the duty ratio of the valve, defined as the time in the on position divided by the switching period, the mean flow and mean pressure are controlled, creating a virtually variable displacement control for any hydraulic pump, motor, or linear actuator.

The promising area of hydraulic hybrid vehicles lacks a variable pump/motor unit that is highly efficient across a wide displacement range, lightweight, and capable of four-quadrant operation, defined as operating as a pump and a motor in both rotational directions [10,11]. Through the use of a high-speed three-way switching valve and a four-way directional control valve, any fixed displacement hydraulic motor can be operated in all four quadrants, given that flow paths prevent cavitation. In the simplified hydraulic circuit diagram of a series hydraulic hybrid vehicle shown in Fig. 1, the pressure is determined by the accumulator state of charge and the high-speed valve modulates the effective displacement and thus the torque of the pump/motor. The directional control valve reverses the torque direction. In the series hydraulic hybrid, to apply torque to the axle, the duty ratio is increased and high pressure fluid from the accumulator and engine driven pump is sent to the motor for a large fraction of each switching period. If the operator wishes to coast and then begin to decelerate, the duty ratio is decreased to 0, the four-way directional control valve is switched to change the torque direction, and the duty ratio is again increased, pumping high pressure fluid into the accumulator.

The primary barrier to efficient switch-mode hydraulic circuits is the limitations of current valve technology. Numerous valve architectures have been proposed for high-speed switching of hydraulic and pneumatic circuits. A large portion of these previous designs, including solenoid valves [7,12], poppet valves [13], and linear spool valves [4,14], require oscillating a mass to achieve the switching operation. As the frequency of operation is increased, significant inertial forces are required to reverse the direction of the mass, resulting in high energy requirements.

A second category of previous valve designs use continuous rotation of a spool to create the valve function. Works at the University of Minnesota and by Cyphelly et al. utilized a rotating spool with a helical profile. In these designs, the pulse width modulated (PWM) frequency is set by the angular velocity of the spool and the duty ratio is set by moving the spool axially with reference to fixed input orifices [6,15]. The University of Minnesota design utilized fluid forces to spin the spool using inlet and outlet turbines [6]. Lu et al. described a flow dividing valve with a constant velocity rotor and three stators. The duty ratio was modulated by changing the angle between the external stators [16]. Royston and Singh presented the design of a pneumatic rotary valve that utilized a phase shift between two sleeves with an internal spool to provide the switching [17]. These last two designs are similar to a kinematic inversion of our valve design. Our design differs from these previous works in that it is a disk style where the fluid travels axially through the valve disks. This elimi-

Contributed by the Dynamic Systems Division of ASME for publication in the JOURNAL OF DYNAMIC SYSTEMS, MEASUREMENT, AND CONTROL. Manuscript received September 25, 2008; final manuscript received June 10, 2010; published online November 23, 2010. Assoc. Editor: Saeid Habibi.

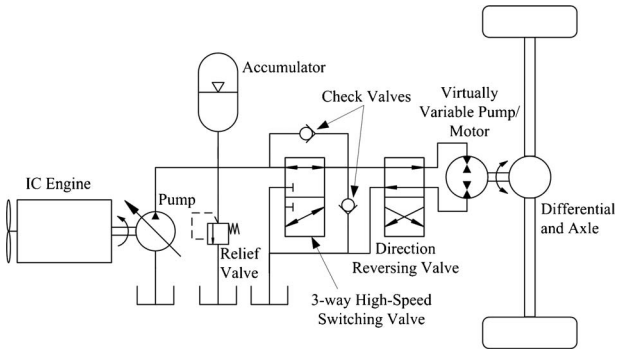

Fig. 1 Hydraulic circuit for a series hydraulic hybrid vehicle with four-quadrant operation of a fixed displacement pump/motor to make a virtually variable displacement unit. The high-speed three-way valve controls the virtual displacement and thus the torque, while the four-way directional valve controls the torque direction. The check valves are used to minimize pressure spikes during valve transitions, as discussed in Sec. 2.2.

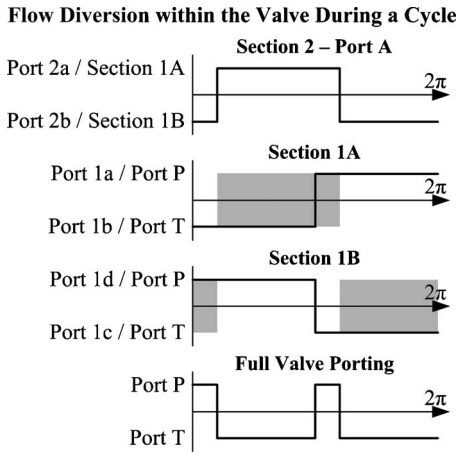

Fig. 3 Plot of the flow diversion in the various sections of the valve during a full rotation for a given phase shift. Note that sections 1A and 1B remain synchronized during operation. Shifting the phase angle between the tier 1 sections and section 2 controls the duty ratio of the valve, observable in the bottom plot of the figure. The port labels correspond to those in Fig. 2. Gray areas denote when section 2 is receiving flow from the tier 1 section.

nates the pumping created in a radial exit rotary valve while also maintaining internal clearances through a hydraulic thrust bearing instead of through manufacturing tolerances and thermal expansion.

This paper presents the concept of a phase-shift high-speed hydraulic valve for switch-mode hydraulic circuit control. Section 2 introduces the concept, architectural options, and a discussion of the valve actuation. Section 3 presents an analysis of the disk style architecture with focus on the forms of energy loss. Section 4 presents the results of the analysis, followed by the discussion of the results in Sec. 5 and concluding remarks in Sec. 6.

2 Method of Approach

2.1 Concept. The novel valve, seen conceptually in Fig. 2, uses a phase shift between flow diverting tiers to achieve a pulsed flow with a variable duty ratio. In the first tier, continuous rotation of the valve spools in each section directs flow from either the tank or pressure input ports to an output port, providing both inputs an equal on-period. Each output flows from the first tier sections becomes the input to the single second tier of the valve. In the second tier, the two input ports are again connected to the output port for equal on-period. All of the valve sections are synchronized and rotated at the same angular velocity and thus divert the flow at the same frequency. By shifting the phase angle between the first tier sections and the second tier section, a three-way valve is created with ports T, P, and A.

During a single revolution of the valve, two full switches occur. Referencing Fig. 2(*a*), consider the cycle starting with section 1A of the valve just beginning to open port 1a. The flow from port 1a becomes the input to section 2 at port 2a, where it is connected to port A. As the valve sections continue to rotate, shown in Fig. 2(*b*), port 1a is still open; however, port 2a has closed. The flow path now goes from the tank port into section 1B through port 1c, into section 2 through port 2b, and out to port A. Further valve rotation will switch the tier 1 sections, opening ports 1b and 1d and closing ports 1a and 1c. Recalling that the tier 1 sections always remain in phase, the flow from port P will enter port 1d and then be sent to port 2b and finally to port A. The final switch occurs as section 2 transitions for a second time, switching the connection of port A back to the tank branch through ports 1b and 2a. As further illustrated in Fig. 3, the full cycle divides the input

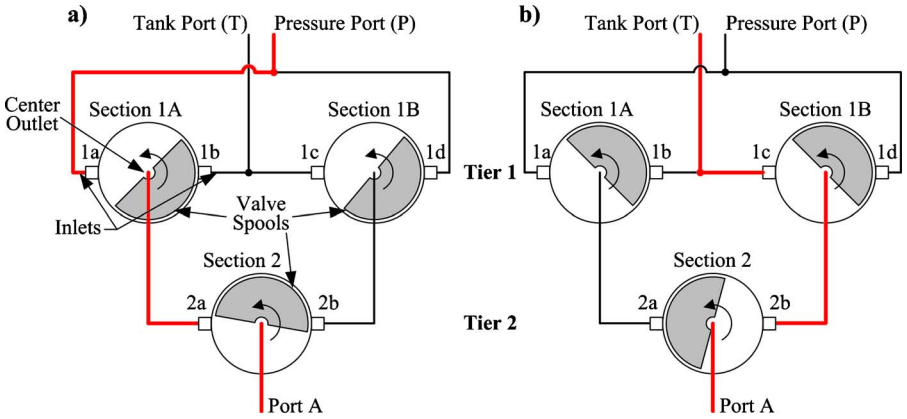

Fig. 2 Schematic representation of the phase shift switching valve at two phases of rotation. Each valve section directs flow from one of the two input ports to a single output port by the rotating valve spool, shown in gray. For clarity, the flow path through the valve for the current positions in subfigures (*a*) and (*b*) is highlighted. Note that subfigure (*b*) has rotated $\pi/2$ rad past subfigure (*a*). The architecture shown creates a two-position three-way valve with two full switches per rotation cycle.

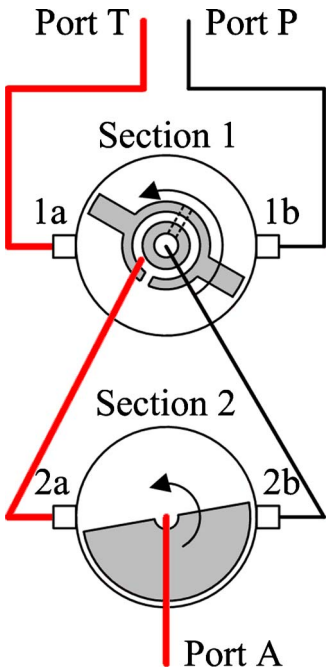

Fig. 4 Schematic of the two tier valve where the previously divided first tier valve sections are combined into a single section. The first tier section has two outputs, port 2b entering the center of the spool and passing through an internal passage to the upper right region of valve section 1 and port 2a entering a groove outside the center of the spool and connecting to the lower left region of the section 1 valve.

flow into four pulsed segments, two going to each of the outputs. Thus, the switching frequency is 2 times the rotational frequency of the valve.

The control of the duty ratio is a unique feature of the phase-shift valve. The duty ratio is continuously variable between 0 and 1, where 0 is defined as full flow to/from the tank, port T, and 1 is defined as full flow to/from pressure, port P. The range of duty ratio is controlled by varying the phase shift between the first and second tiers of the valve from 0 rad to π rad. Note that a negative phase shift or a phase shift beyond π rad also results in a duty ratio between 0 and 1. Controlling the duty ratio through a phase shift enables the function of the valve to be maintained without rigid control on the angular velocity of the valve.

Flow through the phase-shift valve can be bidirectional, allowing regenerative applications. During regeneration, flow from port A is switched between port P and port T. As in generative operation, modulating the duty ratio of the valve controls the regenerative torque of the pump/motor.

2.2 Physical Design. The physical design of the valve can take on various forms. One option includes combining the two first tier valve sections, shown in Fig. 2, into a single valve section. This is accomplished by creating two outlet locations in the first tier section, as shown schematically in Fig. 4. Integrating the two first tier valve sections simplifies the system yet adds an additional leakage path between the neighboring regions of the first tier valve.

The port location on the valve spool can significantly change the architecture of the valve design. Two categories of designs for the rotating valve are an axial flow disk style, similar to Fig. 6, or a radial flow cylinder style, similar to Fig. 2. The radial flow cylindrical valve design rotates a cylindrical spool with slots in the circumferential surface within a sleeve with radial ports. Initial machining of the spool and sleeve establishes the diametral valve clearance. Because the sleeve is often more massive than the rotating spool, care must be taken to prevent seizing the valve due to thermal expansion of the spool during start-up. Due to the radial flow within the rotating cylindrical valve spool, this design acts as a centrifugal pump, requiring additional actuation power and developing a pressure differential across the valve. This pumping behavior makes reversing the flow through the valve difficult.

In the axial flow disk style valve, a disk spool with axial slots rotates past a port plate to divert the flow from one of two input ports to the output port. In contrast to the cylindrical valve design, the clearance between the valve spool and port plate in the disk style valve is established through a force balance of a hydrodynamic thrust bearing, hydraulic pressure, and spring force. By not relying on manufacturing tolerance to establish the valve clearance, the axial flow disk style design lowers manufacturing cost and minimizes the potential of seizing the valve due to thermal expansion. Because the flow is purely axial through the disk spool, pumping does not occur, allowing bidirectional flow through the valve.

Designing the physical valve from the simplified concept schematics for either the cylindrical or disk style phase-shift valve leads to unbalanced fluid forces on the valve spool. To balance the fluid forces, two or more switching sections can be included on each valve spool. Including additional sections provides equal and opposite pressure on the valve spool while increasing the switching frequency for the same rotating frequency.

It should be noted that for a brief period during each cycle, all flow is completely blocked as each valve tier transitions from one inlet port to the other. During these periods, it is necessary to make accommodations to allow for flow continuity. This can include proper placement of check valves, use of small accumulators, or letting the natural compliance of the system cushion the pressure spikes. It needs to be noted that even though these pressure spikes can be managed, they will still create mechanical shock and vibration. In the current work, these pressure spikes are minimized by including check valves in the system, as seen in Fig. 1. During generative operation, when the valve is blocked, flow will pass through the check valve from tank. During regenerative operation, when the valve is blocked, flow will pass through the check valve to the accumulator branch.

2.3 Actuation. Numerous actuation methods exist to rotate the valve spools. Previous work used the inertia of the fluid to spin a turbine shaped cylindrical valve spool [6]. The fluidic actuation alleviates the need for mechanical connection to the valve but introduces a significant pressure drop due to accelerating the fluid to achieve the required inertia. Another contact-free actuation possibility is using the valve spool as the rotor of an electric motor [18]. A more traditional approach is to drive the valve spool with a shaft from an electric motor. A concern with a shaft driven spool, especially for the cylindrical design, is misalignment that can cause off-axis loading, possibly resulting in contact between the spool and the sleeve.

A key to the phase-shift valve is synchronizing the multiple sections of the valve. Rotating the spools with a shaft allows both of the first tier valve sections to be driven by a common shaft, which can be synchronized to a shaft driving the second tier valve section. One option to synchronize the first and second tier shafts is to drive them with a toothed timing belt. By adding adjustable idler pulleys between the valve shafts, the phase angle between the two shafts can be modulated by changing the belt length between the driven pulleys while rotating the shafts at the same angular velocity. Another synchronizing option is to drive each shaft with a servo or stepper motor. The two motors can be operated at the same angular velocity, yet the phase between the two motors can be continuously varied.

3 Modeling and Analysis

To better understand the behavior of the phase-shift valve and the energy losses associated with its operation, a mathematical model is constructed. The primary sources of energy loss in this

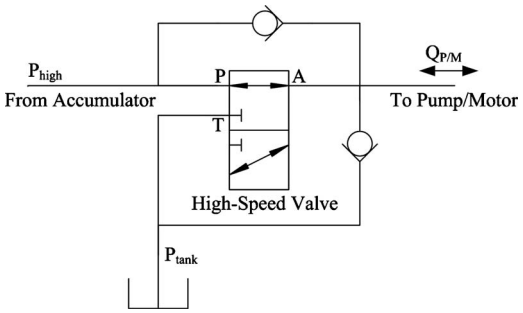

Fig. 5 Simplified high-speed valve and check valves used for analysis purposes. The two check valves have been added to avoid extreme pressure fluctuations occurring when flow is completely blocked during valve transitions.

system are throttling loss during the fully opened and transitioning phases, compressibility losses due to compliance in the hydraulic fluid, viscous frictional forces on the valve spools, and internal leakage within the valve. Other sources of loss that will not be included in this analysis include hysteresis loss in the accumulator, mechanical and volumetric efficiency losses in the pump/motor, and viscous pipe flow losses.

For modeling purposes, a slightly simplified system will be analyzed. Referring back to Fig. 1, it is noted that the two inputs to the high-speed switching valve are at relatively constant pressures, governed by the pressure in the accumulator and the tank. In an application such as driving the wheel of a hybrid vehicle, the shaft speed of the pump/motor is defined by the ground speed of the vehicle. Because this is a fixed displacement pump/motor, the flow rate in and out of the unit is defined by the angular velocity of the shaft. During every switch of the high-speed valve, there is a moment where all flow is completely blocked. If the hydraulic unit was acting as a motor during this time, the inlet of the motor would draw a vacuum and cavitate. Similarly, if the hydraulic unit was acting as a pump, the outlet of the unit would see a large pressure spike. To avoid these issues, two check valves are added to the system, one from outlet of the high-speed valve to the accumulator line and one from the tank to the outlet of the high-speed valve.

A second simplification can be made by observing that during operation, the four-way direction reversing valve is only used to change the torque direction of the motor. As the reversing valve does not influence operation in either the motoring or pumping modes, it can be neglected from the simplified model, other than the additional compressibility losses due to the added fluid volume. The simplified valve circuit used for the analysis is shown in Fig. 5. For analysis purposes, Fig. 2(*a*) is further annotated and presented in Fig. 6 to provide a definition of variables.

With reference to Fig. 6, the key geometry features of the valve are defined. The inlet ports of the valve sections, labeled as 1a-2b, have an inner radius R_i, an outer radius R_o, and a span angle of δ. The disk spool contains an open angle of γ and is sized radially to fully cover the inlet ports. Note that $\delta+\gamma=\pi$, and thus both inlet ports are fully covered two times during every revolution of the spool. For the tier 1 sections of the valve, the angular position of the spool, θ, is referenced to the fully closed position when ports 1b and 1d are beginning to open. Similarly, the angular position of the tier 2 disk is described by $\theta+\alpha$, where α is the phase shift of the valve and varies from 0 rad to π rad.

3.1 Throttling Analysis. A first source of energy loss in the valve is due to throttling the fluid through the ports of the valve in both the fully opened and transitioning states. During every full revolution of the phase-shift valve, two full on-off cycles and thus four switches occur. Through each of these switches, the area of one of the internal valve ports transitions from fully open to fully closed or vice-versa, creating throttling across a variable area orifice. When the duty ratio is at the upper or lower limits, the transition of the first and second tier valve sections overlap, creating throttling across two orifices with changing area.

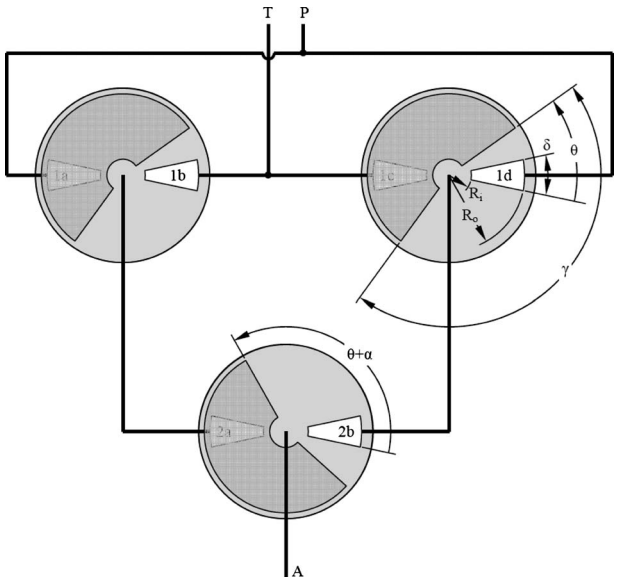

Fig. 6 Annotated schematic of the disk style three-way phase-shift valve geometry. Fluid enters a valve section through the fixed port when it is unobstructed by the valve spool. Fluid leaves each valve section through a center port.

Before calculating the energy loss due to throttling across the fully open and transitioning phases of the valve, an expression must be developed for the area of the internal ports as a function of the angular position of the valve. The reference position for the first tier valve occurs when all ports are fully blocked and ports 1b and 1d, with reference to Fig. 6, are beginning to open. From this reference, the area of ports 1b and 1d can be described by

$$A_{1b,1d}(\theta)=\frac{\theta}{2}(R_o^2-R_i^2) \quad \text{for } 0\le \theta \bmod 2\pi < \delta \tag{1}$$

$$A_{1b,1d}(\theta)=\frac{\delta}{2}(R_o^2-R_i^2) \quad \text{for } \delta\le \theta \bmod 2\pi < \gamma \tag{2}$$

$$A_{1b,1d}(\theta)=\frac{\pi-\theta}{2}(R_o^2-R_i^2) \quad \text{for } \gamma\le \theta \bmod 2\pi < \pi \tag{3}$$

$$A_{1b,1d}(\theta)=0 \quad \text{for } \pi\le \theta \bmod 2\pi < 2\pi \tag{4}$$

where θ modulo 2π maintains the evaluated angle between 0 and 2π for multiple rotations. Similarly, the area of ports 1a and 1c as a function of θ can be described by

$$A_{1a,1c}(\theta)=0 \quad \text{for } 0\le \theta \bmod 2\pi < \pi \tag{5}$$

$$A_{1a,1c}(\theta)=\frac{\theta-\pi}{2}(R_o^2-R_i^2) \quad \text{for } \pi\le \theta \bmod 2\pi < \pi+\delta \tag{6}$$

$$A_{1a,1c}(\theta)=\frac{\delta}{2}(R_o^2-R_i^2) \quad \text{for } \pi+\delta\le \theta \bmod 2\pi < \pi+\gamma \tag{7}$$

$$A_{1a,1c}(\theta)=\frac{2\pi-\theta}{2}(R_o^2-R_i^2) \quad \text{for } \pi+\gamma\le \theta \bmod 2\pi < 2\pi \tag{8}$$

The open area of ports 2a and 2b of the second tier valve section are similarly described with the addition of the phase shift angle α. For example, for port 2b, Eq. (1) becomes

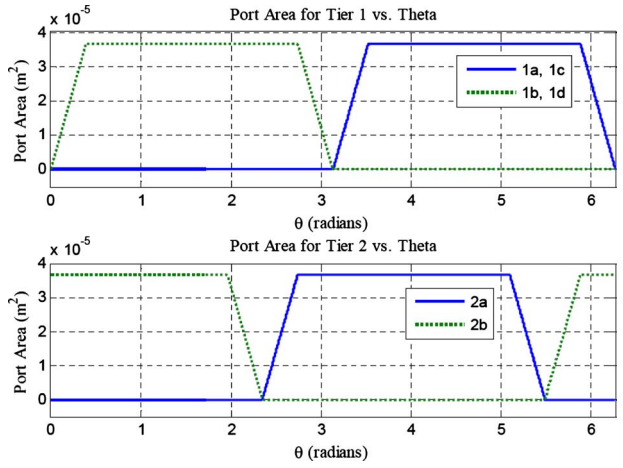

Fig. 7 Open area of the internal ports of the valve as a function of the rotation angle. The areas of the tier 1 ports are displayed in the top plot, while the lower plot shows the area of the tier 2 ports. Note the phase shift of $\pi/4$ rad between the first and second tier ports.

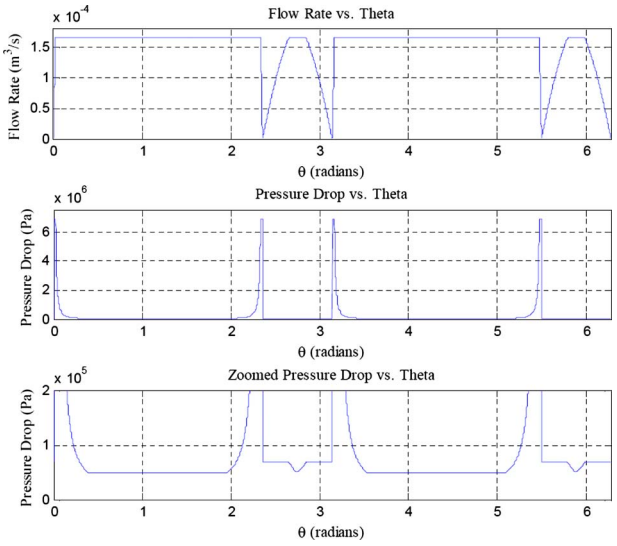

Fig. 8 Flow through and pressure drop across the high-speed valve in motoring mode. The bottom subfigure is a zoomed plot of the center subfigure, highlighting the smaller magnitude pressure drop corresponding to the switches to the tank branch.

$$A_{2b}(\theta) = \frac{\theta + \alpha}{2}(R_o^2 - R_i^2) \quad \text{for } 0 \le (\theta + \alpha) \bmod 2\pi < \delta \tag{9}$$

In the interest of brevity, the remaining area equations for ports 2a and 2b will not be developed. The open area of the ports for a valve rotation with a phase shift of $\pi/4$ rad is presented in Fig. 7. The port angle, δ, in the figure is $\pi/8$ rad, causing the valve transitions periods to nearly overlap between ports 1b, 1d, and 2a.

Due to the use of check valves in the system to provide flow when the high-speed valve is fully blocked, the beginning and end of every switch is characterized by splitting the flow between the high-speed valve and the check valve. For instance, consider the case where port 1d, with reference to Fig. 6, is beginning to open and port 2b is fully open. When port 1d is blocked, full flow passes through either the tank or pressure line check valve, depending on the flow direction. As port 1d begins to open, flow continues to pass through the check valve but also begins to flow through the high-speed valve. During this time, the pressure at port A is defined by the pressure drop across the check valve. As port 1d opens further, the pressure drop across the high-speed valve with full flow reaches equilibrium with the pressure at port A, which is defined by the check valve. When this occurs, full flow passes through the high-speed valve as it continues to open and the check valve closes. This same behavior repeats during closing of the valve.

To determine the flow path behavior through the high-speed valve and the check valves, the pressure drop across the high-speed valve subjected to full flow is first calculated. The full-flow pressure drop across the valve is described by

$$\Delta P_{\text{valve\_full}} = \Delta P_{\text{Tier1}} + \Delta P_{\text{Tier2}} = \frac{\rho}{2}\left(\frac{Q}{C_d A_{\text{Tier1}}}\right)^2 + \frac{\rho}{2}\left(\frac{Q}{C_d A_{\text{Tier2}}}\right)^2 = \frac{\rho Q^2 (A_{\text{Tier1}}^2 + A_{\text{Tier2}}^2)}{2 C_d^2 A_{\text{Tier1}}^2 A_{\text{Tier2}}^2} \tag{10}$$

where $\Delta P_{\text{valve\_full}}$, ΔP_{Tier1}, and ΔP_{Tier2} are the pressure drop due to full flow through the high-speed valve, the first tier of the valve, and the second tier of the valve, respectively, ρ is the mass density of the fluid, Q is the flow rate, C_d is the discharge coefficient of the orifice, and A_{Tier1} and A_{Tier2} are the current area of the first and second tier ports, respectively.

To provide a universal means of determining the pressure drop and flow for the high-speed valve, the flow direction and valve porting need to be considered. When the hydraulic unit is acting as a motor and the tank branch is open or the hydraulic unit is acting as a pump and the pressure branch is open, flow is split between the check valve and the high-speed valve if

$$\Delta P_{\text{valve\_full}} > \Delta P_{\text{check}} \tag{11}$$

where ΔP_{check} is the cracking pressure of the check valve. If the flow is split between the high-speed valve and the check valve, the pressure drop across the high-speed valve is simply

$$\Delta P_{\text{valve}} = \Delta P_{\text{check}} \tag{12}$$

When the hydraulic unit is acting as a motor and the pressure branch is open or acting as a pump and the tank branch is open, flow is split between the check valve and the high-speed valve if

$$\Delta P_{\text{valve\_full}} > P_{\text{high}} - P_{\text{tank}} + \Delta P_{\text{check}} \tag{13}$$

If the flow is split for this case of flow direction and valve porting, the pressure drop across the high-speed valve is described by

$$\Delta P_{\text{valve}} = P_{\text{high}} - P_{\text{tank}} + \Delta P_{\text{check}} \tag{14}$$

For cases where the full flow passes through the high-speed valve, defined by not meeting the above inequalities for the given cases, the pressure drop across the valve is described by Eq. (10).

The calculation of the flow through the high-speed valve and check valve is simpler as it is universal for all situations. By rearranging Eq. (10), the flow through the high-speed valve is described by

$$Q_{\text{valve}} = C_d A_{\text{Tier1}} A_{\text{Tier2}} \sqrt{\frac{2\Delta P_{\text{valve}}}{\rho (A_{\text{Tier1}}^2 + A_{\text{Tier2}}^2)}} \tag{15}$$

By default, the flow through the check valve is always described by

$$Q_{\text{check}} = Q - Q_{\text{valve}} \tag{16}$$

Plots of the pressure drop across and flow through the high-speed valve when the hydraulic unit is acting as a motor can be found in Fig. 8. Recall that the flow into or out of the pump/motor remains constant throughout the switching period. The decrease in flow through the high-speed valve, seen in the first plot of the figure, corresponds to an increase in flow through one of the check valves. During the transition to the tank branch, which occurs at 2.35 rad, the bottom subfigure shows how the pressure is regu-

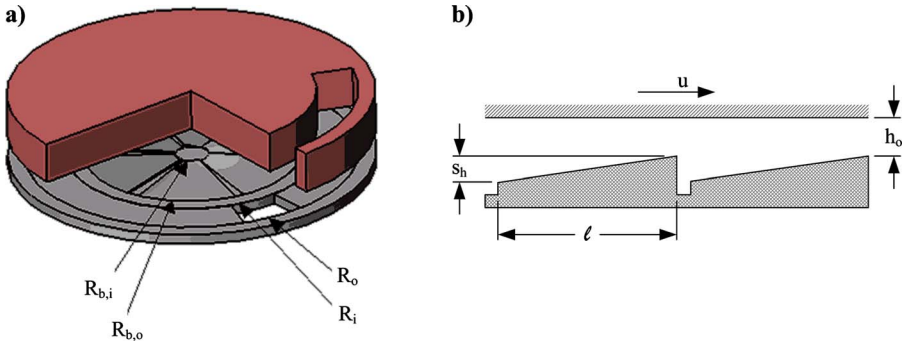

Fig. 9 Thrust bearing schematic with defined dimensional variables. Through a cutaway in the valve disk, subfigure (*a*) shows the thrust bearing pads as arranged on the inside of the valve ports. Subfigure (*b*) gives dimensions for the fixed-incline thrust bearing pads.

lated by the check valve until full flow passes through the high-speed valve. At this point, the pressure drop decreases quadratically. When the hydraulic unit acts as a pump, the pressure regulation by the check valve is most easily observed during the transition to the pressure branch.

The pressure and flow calculations allow the power loss due to throttling to be determined. The throttling loss needs to include losses through both the high-speed valve and the check valve. The instantaneous throttling power loss is described by

$$\text{Power}_{\text{throttling}} = \Delta P_{\text{valve}} Q_{\text{valve}} + \Delta P_{\text{check}} Q_{\text{check}} \tag{17}$$

3.2 Compressibility Analysis. A second source of loss is due to the compressibility of the fluid subjected to fluctuating pressure. During every valve transition to the pressure port, the inlet volume of the hydraulic pump/motor is exposed to high pressure and thus, the fluid density increases. As the valve switches to the tank port, the energy put into increasing the density of the fluid is lost as it decompresses while returning to tank pressure. The volume of hydraulic fluid exposed to this fluctuating pressure, labeled as the inlet volume, includes a portion of the internal volume in the pump/motor, the internal volume of one path of the four-way switching valve, the volume leading to the check valves, a portion of the internal volume in the high-speed valve, and any connecting fluid passages.

The bulk modulus of a fluid describes the reduction in volume due to an applied pressure. The bulk modulus strongly depends on the entrained air content of the fluid as well as the fluid pressure and temperature. A literature search reveals multiple bulk modulus models of varying complexity [19–21]. A relatively simple approach presented by Akers et al. uses the compressibility of the air and the oil separately in an estimation of the effective bulk modulus [19]. Using this approach, the effective bulk modulus can be estimated by

$$\beta_e = \frac{1}{\dfrac{1-R}{\beta_{\text{oil}}} + \dfrac{R}{P_{\text{high}} \cdot k}} \tag{18}$$

where β_e is the effective bulk modulus, β_{oil} is the bulk modulus of air free oil, R is the entrained air content by volume at atmospheric pressure, and k is the ratio of specific heats for air. A comparison of this method with that by Yu et al. reveals a difference of less than 2% at the operating conditions of interest [20].

From the definition of bulk modulus, the change in volume due to every switch from the tank branch to the pressure branch can be described by

$$\Delta V = \frac{(P_{\text{high}} - P_{\text{tank}}) V_{\text{inlet}}}{\beta_e} \tag{19}$$

where ΔV is the change in volume and V_{inlet} is the inlet volume. Finally, the energy loss during each switch due to fluid compression is

$$E_{\text{comp}} = (P_{\text{high}} - P_{\text{tank}}) \Delta V \tag{20}$$

3.3 Thrust Bearing and Viscous Friction Analysis. A prime advantage of an axial flow disk style valve is that the spool to port clearance is created and maintained by fluid forces and not manufacturing tolerances and thermal expansion as in a cylindrical spool style valve. The fluid forces required to maintain the desired valve clearance can be created with either a hydrostatic or a hydrodynamic bearing. For a first analysis, this paper will consider a hydrodynamic thrust bearing as it does not require auxiliary pumping. This section will develop the equations to model a hydrodynamic bearing and predict the energy losses due to viscous forces in the thrust bearing, around the circumference of the valve disk, and across the switching surface of the valve.

A hydrodynamic thrust bearing creates an axial force on a rotating shaft by wedging a fluid into a smaller clearance area through viscous forces, creating an increase in pressure acting on the axial face of the shaft. Numerous geometries can be used to create a hydrodynamic thrust bearing including parallel step sliders, curved sliders, fixed-incline sliders, and pivoting-incline sliders that adjust the angle of the slider based on the axial force. This paper will focus on the fixed-incline slider geometry as it provides an intuitive understanding and minimizes side leakage compared with the parallel step slider [22,23]. As can be noted in Fig. 9(*a*), the thrust bearing pads are located inside of the valve ports. The dimensions of the bearing pad are provided in Fig. 9(*b*).

The solution to the Reynolds equation for hydrodynamic thrust bearings requires numerical form for three-dimensional analysis. By neglecting flow in the radial direction, known as side leakage, analytical solutions are possible [23]. A further simplification is made by assuming that the viscosity of the fluid is constant across the bearing pads. Although viscosity is a function of both temperature and pressure, the error created by this assumption is usually small if the temperature rise is not significant [24]. This paper will present a two-dimensional analytical approach to provide insight into the physics of the fluid behavior.

The analysis will consider a single pad of the thrust bearing in two dimensions, as shown in Fig. 9(*b*). The axial force applied to the thrust bearing is a result of the pressure differences applied to the axial surfaces of the valve disk and can be represented as follows:

$$F_{\text{axial}} = \Delta PA = (P_{\text{high}} - P_{\text{tank}})\frac{2\pi - \gamma}{2}(R_o^2 - R_i^2) \tag{21}$$

where F_{axial} is the total axial force on the valve. It does need to be noted that the pressure applied to the bearing is cyclic due to the pressure changing within the valve. For a worst case scenario of the bearing torque requirements, this analysis will use the full continuous pressure. The normal load per pad per unit width of the pad, w_{pad}, is described by

$$w_{\text{pad}} = \frac{F_{\text{axial}}}{N(R_{b,o} - R_{b,i})} \tag{22}$$

where N is the number of thrust bearing pads and $R_{b,o}$ and $R_{b,i}$ are the outer and inner radius of the thrust bearing pads respectively [23]. A dimensionless normal load-capacity is defined as follows:

$$W = \frac{w_{\text{pad}} s_h^2}{\eta u \ell^2} \tag{23}$$

where s_h is the height of the inclined plane of the thrust bearing, η is the absolute viscosity of the fluid, u is the velocity at the center of the pad, and ℓ is the chordal length of the pad center [23]. The linear velocity is calculated by $u = \omega(R_{b,o} + R_{b,i})/2$, where ω is the angular velocity of the valve disk.

From the Reynolds equation, the normal load-capacity can be equated to the film thickness ratio

$$W = 6\ln\left(\frac{H_o + 1}{H_o}\right) - \frac{12}{1 + 2H_0} \tag{24}$$

where H_{o} is the film thickness ratio, which is defined as $H_o = h_o/s_h$, where h_{o} is the outlet film thickness [23]. H_{o} in Eq. (24) cannot be solved for directly, so a numerical or iterative approach is required.

The viscous frictional force of the thrust bearing is composed of pressure acting against the inclined plane and viscous shear force. The viscous frictional force can be expressed as a ratio to the normal load through a friction coefficient, μ, as follows [23]:

$$\mu = \frac{2s_h \ln\left(\frac{H_o}{H_o + 1}\right) + \frac{3s_h}{1 + 2H_o}}{3\ell \ln\left(\frac{H_o}{H_o + 1}\right) + \frac{6\ell}{1 + 2H_o}} \tag{25}$$

The viscous torque required by the shaft is

$$T_{\text{viscous}} = \mu W \frac{(R_{b,o} + R_{b,i})}{2} \tag{26}$$

To minimize the viscous torque required to spin the valve disk, Eq. (24) can be iteratively solved for the film thickness ratio while varying the height of the inclined step in Eq. (23). This allows a minimum to be found for the viscous torque, as shown in Fig. 10. The minimum value in torque at a step height of 15 μm corresponds to an outlet film thickness, $h_{\text{o}} = 7.2$ μm. Performing a formal optimization on all of the variables would enable the global minima to be found, further reducing energy loss.

In addition to the thrust bearing, viscous drag is also created around the circumference of the rotating valve disk. This viscous drag can be modeled with Petroff's equation for no-load torque [25],

$$T_{\text{journal}} = \frac{2\pi\omega\eta t R_c^3}{c} \tag{27}$$

where T_{journal} is the torque applied to the circumference, t is the axial thickness of the valve disk, R_c is the outer diameter of the valve disk, and c is the radial clearance.

The final viscous energy loss that will be included in this analysis is the shearing of the fluid on the face of the valve disk in the switching area. The area this viscous force acts upon extends from the inner radius to the outer radius of the valve ports and angularly

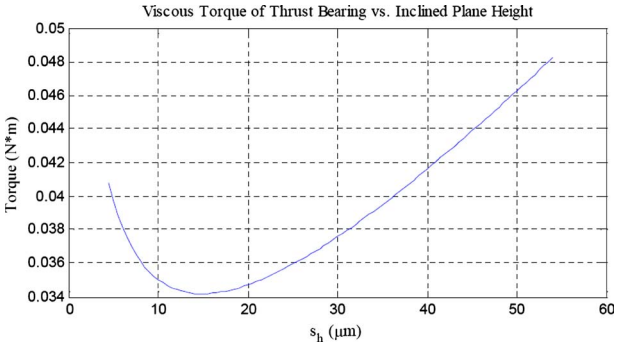

Fig. 10 A plot of the viscous torque due to the hydrodynamic thrust bearing as a function of the height of the inclined plane. Note that the torque required increases significantly when departing from the minima at s_h=15 μm.

across the blocked portion of the valve, except for the exposed area of an inlet port. From Newton's postulate, the frictional torque on the valve disk is

$$T_{\text{plate}} = Fr = \frac{\eta A u}{h_p} r = \int_{\theta=0}^{\theta=\pi} \int_{r=R_i}^{r=R_o} \frac{\eta(r \cdot dr \cdot d\theta)(\omega r)}{h_p} r = \frac{\pi\omega\eta}{4h_p}(R_o^4 - R_i^4) \tag{28}$$

where h_p is the plate film thickness in the port area. From the viscous torque equations for the thrust bearing, valve disk circumference, and valve disk, the total viscous power loss due is calculated,

$$\text{Power}_{\text{viscous}} = (T_{\text{viscous}} + T_{\text{journal}} + T_{\text{plate}})\omega \tag{29}$$

Two closing notes must be made about the axial thrust bearing design. Due to the geometry of the valve presented above, the pressure forces will create side loading of the valve disk, causing the valve disk to rotate perpendicular to the axis of rotation. As discussed in Sec. 2.2, pressure balancing can be achieved by utilizing opposite pairs of ports in each valve subsection; for example, section 1A would have alternating ports 1a, 1b, 1a, and 1b. Second, when the port to tank is open and the port to pressure is blocked, the axial force on the valve disk will reverse direction. This force can be reacted by a constant pressure interior land on the valve disk. The geometry and analysis above were simplified from the required physical design for illustrative purposes.

3.4 Leakage Analysis. The final form of energy loss included in this analysis is the internal leakage within the valve. Two primary leakage paths exist within each valve section, from the blocked port to the unblocked section and from the unblocked section to the center thrust bearing region. With reference back to Fig. 6, leakage from the blocked port to the unblocked sector can travel circumferentially in both the clockwise and counterclockwise directions. At all times, the absolute value of the pressure difference between the blocked port and the open sector is $P_{\text{high}} - P_{\text{tank}}$, although the pressure gradient changes direction with each valve switch.

During the majority of the valve disk rotation, the length of the flow path is substantial, allowing the leakage to be modeled as laminar flow between two parallel plates. However, when the valve is near a transition, the length of the flow path approaches zero, causing a parallel plate flow model to predict infinite flow. While this flow transition is complex, a simplifying assumption will be made that the short length flow can be modeled as orifice flow. By setting the orifice flow equal to the parallel plate flow, the flow path length of flow transition and thus the angle of flow transition can be determined,

$$Q_{\text{orifice}} = Q_{\text{plate}}$$

Table 1 Dimensions and properties of the example valve. Note that the three sections of the valve have identical dimensions.

Property description	Symbol	Value
Inner radius of valve ports	R_i	15 mm
Outer radius of valve ports	R_o	20 mm
Angular port width	δ	$\pi/8$ rad
Angular width of open sector of valve disk	γ	$7\pi/8$ rad
Inner radius of thrust bearing pads	$R_{b,i}$	2 mm
Outer radius of thrust bearing pads	$R_{b,o}$	13 mm
Number of thrust bearing pads	N	3
Outer radius of valve disk	R_c	22 mm
Axial thickness of valve disk	t	5 mm
Radial clearance of valve disk	c	0.8 mm
Film thickness in porting area of valve disk	h_p	12 μm
Inlet volume exposed to fluctuating pressure	V_{inlet}	6.8×10^{-6} m^3
Switching frequency	f_{switch}	100 Hz
Rotating frequency	f_{rotate}	50 Hz
Pressure of the source/accumulator	P_{high}	6.9 MPa
Pressure of the tank	P_{tank}	101 kPa
Pressure drop across check valve	ΔP_{check}	69 kPa
Flow rate to/from the pump/motor	Q	1.67×10^{-4} m^3/s
Density of the hydraulic fluid	ρ	876 kg/m^3
Absolute viscosity of the hydraulic fluid	η	0.0387 Pa s
Bulk modulus of air free hydraulic fluid	β	1.9 GPa
Entrained air by volume at atmospheric pressure	R	1%

$$C_d A\sqrt{\frac{2}{\rho}\Delta P}=\frac{2bh^3\Delta P}{3\eta L} \tag{30}$$

where Q_{orifice} and Q_{plate} are the orifice flow and parallel plate flow, respectively, b is the width, h is half of the distance between the plates, $\Delta P=P_{\text{high}}-P_{\text{tank}}$, and L is the flow length. By definition, $h_p=2h$. By recognizing that $A=2bh$ and $L=\theta(R_i+R_0)/2$, the resulting angle of flow transition is

$$\theta_{\text{trans}}=\frac{2h^2}{3\eta C_D(R_i+R_o)}\sqrt{\frac{\rho\Delta P}{2}} \tag{31}$$

where θ_{trans} is the rotation angle where the flow transitions from orifice flow to parallel plate flow. Further recognizing that the flow transition occurs four times per revolution and using the definition of $\omega=d\theta/dt$, the volume of leakage flow per revolution is

$$V_{\text{circum}}=4\int_{t=o}^{t=\pi/2\omega}Q(\theta)dt=\frac{4}{\omega}\int_{\theta=0}^{\theta=\pi/2}Q(\theta)d\theta$$
$$=\frac{4}{\omega}\left[\int_{\theta=0}^{\theta=\theta_{\text{trans}}}Q_{\text{orifice}}d\theta+\int_{\theta=\theta_{\text{trans}}}^{\theta=\pi/2}Q_{\text{plate}}(\theta)d\theta\right] \tag{32}$$

where

$$Q_{\text{plate}}(\theta)=Q_{\text{plate,CCW}}(\theta)+Q_{\text{plate,CW}}(\theta)=\frac{2(R_o-R_i)h^3\Delta P}{3\eta\left(\frac{R_o+R_i}{2}\right)\theta}$$
$$+\frac{2(R_o-R_i)h^3\Delta P}{3\eta\left(\frac{R_o+R_i}{2}\right)(\pi-\theta)} \tag{33}$$

Substituting Eq. (33) into Eq. (32) and integrating yields the circumferential leakage volume per revolution:

$$V_{\text{circum}}=\frac{4}{\omega}\left[C_d A\theta_{\text{trans}}\sqrt{\frac{2}{\rho}\Delta P}+\frac{4(R_o-R_i)h^3\Delta P}{3\eta(R_o+R_i)}\ln\left(\frac{\pi}{\theta_{\text{trans}}}-1\right)\right] \tag{34}$$

Based on the fact that the absolute value of the pressure drop between the blocked port and the unblocked sector remains constant throughout operation, the energy loss per section due to the circumferential leakage is simply the difference between high and tank pressure multiplied by the volume of leakage per revolution.

The second leakage loss in the valve is from the open sector to the thrust bearing. Because the fluid in the thrust bearing is near tank pressure, this flow only occurs when the open sector is at high pressure, which is approximated as $1/2$ of every cycle for each section. The leakage flow to the thrust bearing is modeled as laminar flow between parallel plates. From the flow between parallel plates equation, found on the right side of Eq. (30), the inward radial flow from the open sector to the thrust bearing is expressed as follows:

$$Q_{\text{radial}}=\frac{(R_i+R_{b,o})\gamma h^3(P_{\text{high}}-P_{\text{tank}})}{3\eta(R_i-R_{b,o})} \tag{35}$$

The average power loss due to the inward radial leakage flow is the difference between high and tank pressure multiplied by half the volumetric flow rate calculated in Eq. (35).

4 Results

To provide a quantitative comparison of the contribution of each form of energy loss and to create a baseline valve efficiency, an example design is provided. It must be noted that the example design is by no means optimized; it is strictly for illustrative purposes. The example valve is designed for a source pressure of 6.9 MPa (1000 psi) and a flow rate of 10 l/min (2.6 gpm). These parameters were selected based on an available hydraulic power supply and the desire to compare the results of this paper with experimental work in the future. For a hydraulic hybrid passenger car, realistic parameters are a pressure of 35 MPa (5000 psi) and a flow rate of 150 l/min (40 gpm). The valve will have a switching frequency of 100 Hz and is fully adjustable from a duty ratio of 0

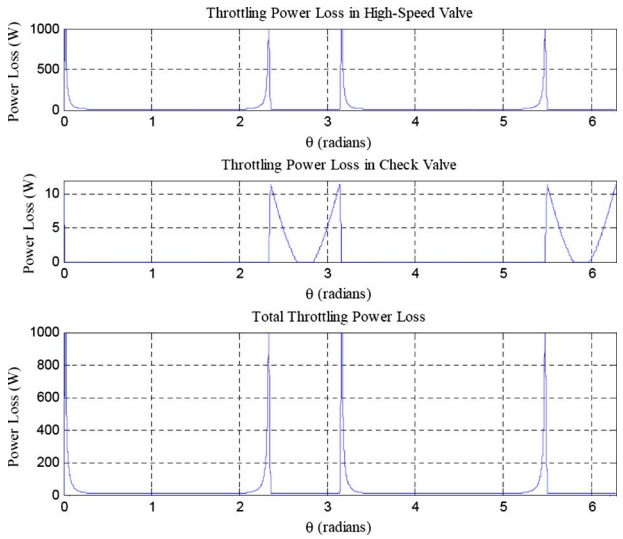

Fig. 11 Instantaneous power loss due to throttling for a single valve rotation when the hydraulic unit is acting as a motor. Note that the throttling through the high-speed valve during the opening and closing of the pressure branch dominates the power loss contributions.

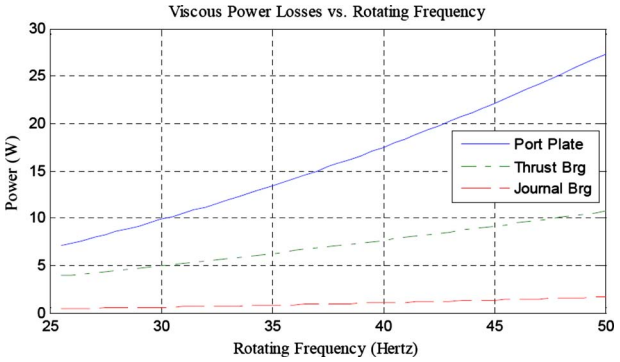

Fig. 12 The viscous power loss components as a function of valve disk rotating frequency. Note the dominance of the viscous losses on the port plate due to the larger acting radius.

to 1. The two tier valve will use three identical rotating disk sections. The full specifications of the valve sections can be found in Table 1.

4.1 Throttling Loss Results. As discussed in Sec. 3.1, flow is throttled across the high-speed valve and a check valve during each switching transition, dissipating energy. Multiplying the pressure drop across the valves by the flow rate allows the instantaneous power loss to be calculated. As seen in Fig. 11, high magnitude power loss is seen for a short period of time through the high-speed valve. The magnitude of the throttling power loss through the check valve is approximately an order of magnitude lower than the high-speed valve.

The energy loss due to throttling is independent of the switching frequency. While more throttling events will occur with an increase in the switching frequency, the duration of these events becomes shorter, creating independence. For the design example, the average power loss due to throttling is 32.7 W.

4.2 Bulk Modulus Loss Results. Pressure fluctuations in the slightly compressible fluid within the inlet volume of the pump/motor leads to compressibility energy loss. The inlet volume is estimated at 6.8 cm^3 and includes the volume between the first and second tiers of the valve, the four-way directional valve, and the passage leading to the inlet of the pump/motor. For this estimate, a manifold is used to mount the high-speed valve, check valves, and directional valve directly to the pump/motor housing to reduce volume. With 1% air entrainment in the hydraulic fluid by volume and a pressure of 6.9 MPa, the effective bulk modulus is approximately 3 times less than the bulk modulus of air free fluid.

The compressibility energy loss is linearly related to the switching frequency as it results from releasing the energy used to compress the fluid during every switch from high to tank pressure. The compressibility energy loss for the example design is 0.48 J per switching cycle. Note that if the air entrainment increased to 5% by volume, the compressibility energy loss would increase to 1.75 J per switching cycle.

4.3 Thrust Bearing Design and Viscous Loss Results. The torque requirements of the hydrodynamic thrust bearing are a significant energy sink. For the design example geometry, the power loss due to the thrust bearing torque is 10.7 W for each valve section. The numerous factors influencing the torque requirements of the thrust bearing make a formal optimization important for a final design. The power loss for the circumferential journal bearing friction is 2.18 W, and the frictional power loss across the porting area of the valve disk is 27.3 W.

The viscous friction energy loss is a function of the valve disk rotating frequency. The two purely viscous losses, the circumferential journal bearing and the port plate, exhibit a quadratic relationship between power consumption and rotating frequency, as seen in Fig. 12. The pressure and viscous forces of the thrust bearing create a superlinear relationship between power loss and rotating frequency. The figure also demonstrates the dominance of the friction of the port plate compared with the other two forms of loss. The quadratic relationship between radius and power loss makes this viscous shearing on this larger radius overriding.

4.4 Leakage Loss Results. The two forms of leakage within the valve decrease the effective flow rate and thus create a loss of energy. The circumferential leakage path length and thus flow rate vary with the valve angle. The average power loss due to the circumferential leakage is 11.9 W for the design example. The second form of leakage, radial leakage into the thrust bearing, occurs when the open sector of the valve is at high pressure. This occurs one-half of the time for the tier 1 sections and varies for the tier 2 sections based on the duty ratio. Assuming a duty ratio of 0.5, the average power loss due to the radial leakage is 24.8 W. All of the leakage energy loss terms are independent of the operating frequency of the valve.

4.5 Power Loss Summary. The design example is provided as a way of comparing the various components of energy loss in the high-speed phase-shift valve. A summary of the power loss, provided in Table 2, demonstrates a nonoptimized total power loss of 311 W. At a duty ratio of 1, describing connection of the pump/motor port to the pressure port 100% of the time, 1152 W of hydraulic power is transmitted through the valve. Thus, at a duty ratio of 1, the valve efficiency is 73%. At a duty of 0.75, 864 W of hydraulic power is transmitted for a valve efficiency of 64%. Be-

Table 2 A summary of the power loss components for the design example. Note that the viscous friction and leakage losses are multiplied by the number of sections in the valve.

Average power loss summary	
Throttling losses	32.7 W
Compressibility loss	48.2 W
Viscous friction losses	3×40.2 W
Leakage losses	3×36.6 W
Total	311.3 W

cause the majority of the energy losses are independent of duty ratio, the valve efficiency decreases rapidly as the transmitted hydraulic power decreases.

5 Discussion

The results of the analysis through the design example demonstrated the contributions of each power loss factor. All of these sources of loss, with the exception of the viscous friction loss, are hydraulic energy losses, directly decreasing the hydraulic power output in terms of pressure or flow. Because the basic design of the phase-shift disk valves requires external actuation to spin the valve disks, the viscous friction loss is an external loss. This external loss would be the energy generated by an electric motor, auxiliary hydraulic motor, or other form of rotary actuator.

The dependence of the different forms of power loss on the switching or rotating frequency of the valve is important to minimizing the total energy loss. Both the throttling loss and the leakage losses are pressure driven and independent of the operating frequency of the valve. The bulk modulus, or compressibility loss, is directly proportional to the switching frequency of the valve. The final loss, viscous friction, is proportional to the square of the rotating frequency of the valve.

Because the design example was for illustrative purposes only and was not optimized, there exists numerous ways to decrease total valve energy loss. Some of these options include the following.

- As the viscous friction is a function of the rotating frequency, viscous energy loss can be decreased by increasing the number of ports in each valve section. For example, by doubling the number of ports, the same switching frequency can be obtained with $1/2$ of the rotating speed of the valve. This effectively decreases the viscous friction losses by a factor of four. Creating multiple ports also allows the valve spool forces to be balanced, eliminating side loads.
- As discussed in Sec. 2.2 and as illustrated in Fig. 4, the first tier valve sections can be combined into a single section. This will reduce the number of rotating valve disks and thus the multiplying factor on the viscous friction losses and leakage losses. Note that this approach will add an extra leakage path within the first tier valve that will need to be managed.
- Through careful design and integration of the valve and the pump/motor, the inlet volume can be reduced, reducing the compressibility loss.
- Because the effective bulk modulus of the hydraulic fluid is strongly a function of the air content, minimizing air entrainment is critical to minimizing compressibility loss.
- The inlet ports are sized for a specific pressure drop at full flow. Through an optimization, it might be appropriate to increase this pressure drop by decreasing the valve radius, which decreases the viscous forces.
- An opportunity exists for optimizing the relationship between the angle of the inlet port, δ, and the radial length of the port. As the port angle is increased, the transition time of the switch increases, increasing throttling loss; yet, as the port angle increases, the radial length decreases, decreasing the viscous losses. In addition, the radial length affects the area the pressure acts upon and thus the load reacted by the thrust bearing.
- The design of the thrust bearing is relatively complex and allows ways to decrease energy loss. One option from a valve geometry standpoint is integrating the thrust bearing pads and the valve ports into the same radial area. For example, four inlet ports could be evenly spaced around the valve with two thrust bearing pads between each inlet port. During operation, four of the thrust bearing pads would be active and four would be inactive due to the open sector exposing the pads. This would allow the valve radius to be drastically decreased, decreasing viscous friction forces. The thrust bearing geometry also requires careful design to minimize loss, including considering a parallel step or a pivoting incline pad, design of the pad geometry, and creating methods to minimize side leakage.

6 Conclusion

Switch-mode valve control of hydraulic circuits enables a new realm of capabilities. By operating close to completely on or off at all times, traditional throttling approaches of control are eliminated, improving system efficiency. Furthermore, by adding a high-speed valve and an accumulator to a circuit, any hydraulic actuator can have virtually variable displacement, including linear actuators and pump/motor designs that are difficult to make physically variable such as gear or gerotor units. By including a directional switching valve, pump/motors can operate overcenter in all four quadrants.

The novel phase-shift valve concept is a promising valve architecture for switch-mode circuits. The valve design is compact, maintaining the high power density characteristics of hydraulics. The phase shift concept can be easily scaled for various flow requirements and is easily actuated due to independent control of the PWM frequency and the duty ratio. The disk style design creates valve clearance using a hydrodynamic thrust bearing, eliminating changes in clearance due to manufacturing tolerance stack-up or thermal expansion. Due to the axial flow through the disk style valve, no pumping is created, allowing bidirectional flow.

A preliminary analysis and design example demonstrated the feasibility of a 100 Hz phase-shift disk style valve with a flow rate of 10 l/min. While the example design has a predicted efficiency of 73% at a duty ratio of 1 and 64% at a duty ratio of 0.75 from the preliminary analysis, the efficiency of the valve can be greatly improved in numerous ways. Further analysis and design is required for both the valve and the switch-mode system to realize full potential.

The high-speed valve design requires a formal optimization of the numerous parameters to minimize the total energy loss. Detailed analysis is also required in a few specific areas including: (1) A computational fluid dynamics analysis of the transition in leakage behavior from laminar plate flow to orifice as the length of the flow path changes during valve rotation. (2) Numerical bearing analysis that includes radial flow, fluid temperature analysis, and fluid flow requirements. Analyzing the merits of the various thrust bearing pad designs for this application is also an important work. (3) Through clever design, the pressure spikes during valve transition can likely be minimized to reduce throttling loss. (4) Finally, numerous details need to be addressed regarding the physical design including the drive mechanism, valve sealing, and the overall manufacturability with attention to the thrust bearing pads.

Because the high-speed valve is just one component of switch-mode hydraulic circuit, system design and analysis is important. While the design example in this paper arbitrarily selected a switching frequency of 100 Hz, determining the required operating frequency for the system of interest is important. The switching frequency primarily influences the system response time and the pressure ripple seen at the hydraulic actuator. Also at the system, design level is reducing the fluid volume between the valve and the hydraulic actuator to improve the system response and lower the compressibility loss. Another area that must be investigated is the opening and closing time of the check valves to ensure smooth operation during valve transition periods. A final component that is critical to operation is the hydraulic accumulator, which must be sized and have appropriate pre-charge for the desired system operation.

In summary, switch-mode valve control is an important breakthrough for hydraulics and is enabled by the phase-shift high-

speed valve. The phase shift concept has much potential, yet requires further work in a few specific areas and overall optimization to meet its full potential.

References

[1] Li, P. Y., Li, C. Y., and Chase, T. R., 2005, "Software Enabled Variable Displacement Pumps," ASME International Mechanical Engineering Congress and Exposition, Orlando, FL, Vol. 12, pp. 63–72.

[2] Mohan, N., Robbins, W. P., and Undeland, T. M., 1995, *Power Electronics: Converters, Applications and Design*, Wiley, New York.

[3] Cao, J., Gu, L., Wang, F., and Qui, M., 2005, "Switchmode Hydraulic Power Supply Theory," ASME International Mechanical Engineering Congress and Exposition, Orlando, FL, pp. 85–91.

[4] Rannow, M. B., Tu, H. C., Li, P. Y., and Chase, T. R., 2006, "Software Enabled Variable Displacement Pumps—Experimental Studies," ASME International Mechanical Engineering Congress and Exposition, Chicago, IL.

[5] Tomlinson, S. P., and Burrows, C. R., 1992, "Achieving a Variable Flow Supply by Controlled Unloading of a Fixed-Displacement Pump," ASME J. Dyn. Syst., Meas., Control, **114**, pp. 166–171.

[6] Tu, H. C., Rannow, M., Van de Ven, J., Wang, M., Li, P., and Chase, T., 2007, "High Speed Rotary Pulse Width Modulated On/Off Valve," Proceedings of the ASME International Mechanical Engineering Congress, Seattle, WA, p. 42559.

[7] Muto, T., Yamada, H., and Suematsu, Y., 1990, "PWM-Digital Control of a Hydraulic Actuator Utilizing Two-Way Solenoid Valves," J. Fluid Control, **20**(2), pp. 24–41.

[8] Lumkes, J. H., van Doorn, W., and Donaldson, J., 2005, "The Design and Simulation of a High Force Low Power Actuation System for Camless Engines," ASME International Mechanical Engineering Congress and Exposition, Orlando, FL, pp. 553–561.

[9] Beachley, N. H., and Fronczak, F. J., 1988, "A High Efficiency Multi-Circuit Sequential Apportioning Hydraulic System," National Conference on Fluid Power, Chicago, IL, pp. 141–152.

[10] Karmel, A. M., 1990, "Design and Analysis of a Transmission Hydraulic System for an Engine-Flywheel Hybrid-Vehicle," ASME J. Dyn. Syst., Meas., Control, **112**(2), pp. 253–260.

[11] Van de Ven, J. D., Olson, M. O., and Li, P. Y., 2008, "Development of a Hydro-Mechanical Hydraulic Hybrid Drive Train With Independent Wheel Torque Control for an Urban Passenger Vehicle," International Fluid Power Exposition, Las Vegas, NV, pp. 1–11.

[12] Kajima, T., Satoh, S., and Sagawa, R., 1994, "Development of a High Speed Solenoid Valve," Trans. Jpn. Soc. Mech. Eng., Ser. C, **60**(576), pp. 2744–2751.

[13] Yokota, S., and Akutu, K., 1991, "A Fast-Acting Electro-Hydraulic Digital Transducer," JSME Int. J., Ser I, **34**(4), pp. 489–495.

[14] Cui, P., Burton, R. T., and Ukrainetz, P. R., 1991, "Development of a High Speed On/Off Valve," SAE Technical Paper No. 911815, pp. 21–25.

[15] Cyphelly, I., and Langen, H. J., 1980, "Ein Neues Energiesparendes Konzept Der Volumenstromdosierung Mit Konstantpumpen," Aachener Fluidtechnisches Kolloquium, pp. 42–61.

[16] Lu, X. F., Burton, R. T., Schoenau, G. J., and Zeng, X. R., 1991, "Feasibility Study of a Digital Variable Flow Divider," SAE Technical Paper No. 911816, pp. 27–34.

[17] Royston, T., and Singh, R., 1993, "Development of a Pulse-Width Modulated Pneumatic Rotary Valve for Actuator Position Control," ASME J. Dyn. Syst., Meas., Control, **115**, pp. 495–505.

[18] Phaneuf, C., 2008, *Electric Motor Integration with a Rotary On/Off Valve*, The Cooper Union for the Advancement of Science and Art, New York.

[19] Akers, A., Gassman, M., and Smith, R., 2006, *Hydraulic Power Systems Analysis*, Taylor & Francis, Boca Raton, FL.

[20] Yu, J., Chen, Z., and Lu, Y., 1994, "The Variation of Oil Effective Bulk Modulus With Pressure in Hydraulic Systems," ASME J. Dyn. Syst., Meas., Control, **116**, pp. 146–150.

[21] Totten, G. E., Webster, G. M., and Yeaple, F. D., 2000, "Physical Properties and Their Determination," *Handbook of Hydraulic Fluid Technology*, G. E. Totten, ed., Marcel Dekker, New York.

[22] Constantinescu, V. N., Nica, A., Pascovici, M. D., Ceptureanu, G., and Nedelcu, S., 1985, *Sliding Bearings*, Allerton, New York.

[23] Hamrock, B. J., 1994, *Fundamentals of Fluid Film Lubrication*, McGraw-Hill, New York.

[24] Raimondi, A. A., and Boyd, J., 1955, "Applying Bearing Theory to the Analysis and Design of Pad-Type Bearings," Trans. ASME, **77**(3), pp. 287–309.

[25] Norton, R. L., 2006, *Machine Design—An Integrated Approach*, Prentice-Hall, Englewood Cliffs, NJ.